

 方知库  
Eco-Environmental  
Knowledge Web

# 环境科学

ENVIRONMENTAL SCIENCE

ISSN 0250-3301 CODEN HCKHDV  
HUANJING KEXUE

- 主办 中国科学院生态环境研究中心
- 出版 科学出版社



**2019**

Vol.40 No.3  
第40卷 第3期

目次

2014~2017北京市气象条件和人为排放变化对空气质量改善的贡献评估.....尹晓梅,李梓铭,熊亚军,乔林,邱雨露,孙兆彬,寇星霞(1011)

利用多元线性回归方法评估气象条件和控制措施对APEC期间北京空气质量的影响.....李颖若,汪君霞,韩婷婷,王焱,何迪,权维俊,马志强(1024)

京津冀郊区站点秋冬季大气PM<sub>2.5</sub>来源解析.....王彤,华阳,许庆成,王书肖(1035)

四川省典型工业行业PM<sub>2.5</sub>成分谱分析.....冯小琼,陈军辉,熊文朋,梅林德,徐雪梅,尹寒梅,范武波,姜涛,钱骏,叶宏(1043)

典型物流城市2016年冬季2次污染过程PM<sub>2.5</sub>污染特征及来源解析.....赵雪艳,杨文,王静,刘盈盈,白雯宇,徐艳萍,王歆华,白志鹏(1052)

沈阳市采暖期与非采暖期空气PM<sub>2.5</sub>污染特征及来源分析.....张显,田莎莎,刘盈盈,赵雪艳,余浩,张辉,陈莉,王歆华(1062)

新乡冬季PM<sub>2.5</sub>中金属元素与水溶性离子年际变化及其来源解析.....闫广轩,雷豪杰,张靖雯,唐明双,张佳羽,曹治国,李云蓓,王跃思,樊静,李虎(1071)

烟台市环境受体PM<sub>2.5</sub>四季污染特征与来源解析.....刘童,王晓军,陈倩,温杰,黄渤,朱红霞,田瑛泽,冯银厂(1082)

常州市冬季PM<sub>2.5</sub>中类腐殖质昼夜特征分析.....顾远,李清,黄雯倩,赵竹子,马帅帅,叶招莲(1091)

西北某电子垃圾拆解厂室内外重金属污染特征及暴露风险.....曹红梅,赵留元,穆熙,李尧捷,毛潇萱,黄韬,马建民,高宏(1101)

京津冀一次污染过程的星地同步动态监测分析.....邱昀,李令军,姜磊,王新辉,赵文慧,张立坤,鹿海峰(1111)

中国城市O<sub>3</sub>浓度时空变化特征及驱动因素.....黄小刚,赵景波,曹军骥,宋永永(1120)

基于卫星和地面观测的2013年以来我国臭氧时空分布及变化特征.....张倩倩,张兴赢(1132)

舟山市臭氧污染分布特征及来源解析.....王俏丽,董敏丽,李素静,吴成志,王刚,陈必新,李伟,高翔,叶荣民(1143)

中国建筑涂料使用VOCs排放因子及排放清单的建立.....高美平,邵霞,聂磊,王海林,安小栓(1152)

异戊二烯和甲苯二次有机硫踪物的臭氧非均相氧化.....黄亚娟,曹罡,朱荣淑,欧阳峰(1163)

兰州市农牧业源氨排放清单及其时空分布特征.....栗世学,郭文凯,何昕,朱玉凡,陈强(1172)

成都次降水稳定氢氧同位素特征及水汽来源分析.....胡月,刘国东,孟玉川,张文江,夏成城(1179)

基于TBL模型的闽江口围垦养虾塘水-大气界面CO<sub>2</sub>扩散通量估算.....张逸飞,杨平,赵光辉,李玲,谭立山,全川(1188)

渤海和北黄海有色溶解有机物(CDOM)的分布特征和季节变化.....刘兆冰,梁文健,秦礼萍,唐建辉(1198)

思林水库荧光溶解性有机质的特征、来源及其转化动力学.....劳心宇,原杰,刘瑜, Khan M. G. Mostofa(1209)

厦门湾海滩微塑料污染特征.....刘启明,梁海涛,锡桂莉,胡欣,葛健(1217)

高分辨率监测下的漓江省里断面生物地球化学特征分析.....王奇岗,肖琼,赵海娟,王健力,郭永丽,张清华(1222)

鲜水河断裂带拉花盆地地下水化学特征及控制因素.....何锦,张幼宽,赵雨晴,韩双宝,刘元晴,张涛(1236)

成都市锦江表层水和沉积物中有机磷酸酯的污染特征.....吴迪,印红玲,李世平,王增武,邓旭,罗怡,罗林(1245)

丹江口库区表层浮游细菌群落组成与PICRUS1功能预测分析.....张菲,田伟,孙峰,陈彦,丁传雨,庞发虎,姚伦广,李玉英,陈兆进(1252)

蓝藻水华对太湖水柱反硝化作用的影响.....刘志迎,许海,詹旭,朱广伟,秦伯强,张运林(1261)

基于微生物生物完整性指数的城市河道生态系统健康评价.....苏瑛,许育新,安文浩,王云龙,何振超,楼颖雯,沈阿林(1270)

生物炭添加对湿地植物菖蒲根系通气组织和根系泌氧的影响.....黄磊,梁根坤,梁岩,罗星,陈玉成(1280)

城市不同材料屋面径流的污染负荷特性.....何湖滨,陈诚,林育青,严晗璐,董建玮,陈求稳(1287)

BiOCl-(NH<sub>4</sub>)<sub>3</sub>PW<sub>12</sub>O<sub>40</sub>复合光催化剂制备及其光催化降解污染物机制.....张文海,吉庆华,兰华春,李静(1295)

微米铁复合生物碳源对地下水中1,2-二氯乙烷的高效去除.....吴乃瑾,宋云,魏文侠,王海见,孙仲平(1302)

鸟粪石天然沸石复合材料对水中铅离子的去除.....邓曼君,王学江,成雪君,景焕平,赵建夫(1310)

Ca/Mg负载改性渣渣生物炭对水中磷的吸附特性.....易蔓,李婷婷,李海红,黄巧,杨金娥,陈玉成,杨志敏(1318)

两种生物炭的制备及其对水溶液中四环素去除的影响因素.....程扬,沈启斌,刘子丹,杨小莹,张太平,廖志钟(1328)

静止和水动力扰动状态下铅改性沸石添加对河道底泥磷迁移转化的影响.....俞阳,林建伟,詹艳慧,何思琪,吴小龙,王艳,赵钰颖,林莹,刘鹏茜(1337)

4种磺胺类药物及乙酰化代谢物在污水处理厂的去及机制.....王大鹏,张烟,颜昌宙(1347)

以膜分离为主的物化法对城市污水中污染因子的去除特性分析.....徐婷,李勇,朱怡嘉,薛梦婷,汤同欢(1353)

进水氨氮浓度对生物除磷颗粒系统的影响.....李冬,曹美忠,郭跃洲,梅宁,李帅,张杰(1360)

除磷亚硝化颗粒工艺启动及性能恢复.....李海玲,李冬,张杰,刘博(1367)

CAST工艺高温短程硝化的实现及其除磷性能.....马娟,杨蕊春,俞小军,周猛,陈永志(1375)

不同曝气量和好氧时间下SPNDPR系统处理低C/N城市污水的脱氮除磷性能.....袁梦飞,于德爽,巩秀珍,王晓霞,陈光辉,杜世明,甄建园(1382)

ABR除碳-亚硝化耦合厌氧氨氧化处理城市污水.....李田,曹家炜,谢凤莲,沈耀良,吴鹏,宋吟玲(1390)

室温低氨氮基质单级自养脱氮颗粒污泥启动效能与污泥特性.....谢璐琳,王建芳,钱飞跃,张泽宇,沈耀良,齐泽坤(1396)

不同种泥的厌氧氨氧化反应器的启动及动力学特征.....任君怡,陈林艺,李慧春,秦玉洁,姜雁,王桐屿,周少奇(1405)

降温过程中生物膜CANON反应器的运行特征.....付昆明,廖敏辉,周厚田,付巢,姜婍,仇付国,曹秀芳(1412)

IEM-UF同步分离反硝化系统脱氮特性及种群结构分析.....刘子奇,张岩,马翔山,张博康,曹孟京,陈昌明(1419)

温度对硝化杆菌(Nitrobacter)活性动力学影响.....于雪,孙洪伟,李维维,祁国平,马娟,陈永志,吕心涛(1426)

零价铁和微波预处理组合强化污泥厌氧消化.....牛雨彤,刘吉宝,马爽,李亚明,解立平,魏源送,孟晓山(1431)

牛粪堆肥系统环境因子对抗性基因的影响.....彭磊,王科,谷月,王爱杰(1439)

环境因子对土壤微生物呼吸及其温度敏感性变化特征的影响.....张彦军,郭胜利(1446)

三峡库区典型微生物土壤呼吸及其组分对模拟酸雨的反应.....李一凡,王玉杰,王彬,王云琦(1457)

三峡库区柑橘园施肥量对土壤氮淋失及残留量的影响.....王甜,黄志霖,曾立雄,肖文发,宋文梅(1468)

长期施肥下水稻根际和非根际土壤微生物碳源利用特征.....宁赵,程爱武,唐海明,葛体达,邓扬悟,苏以荣,陈香碧(1475)

不同碳负荷梯度下稻田土壤有机碳矿化特征.....童瑶瑶,王季斐,祝贞科,邓扬悟,陈珊,葛体达,袁红朝,吴金水(1483)

桂林市仙喀斯特湿地水位梯度下不同植物群落土壤有机碳及其组分特征.....徐广平,李艳琼,沈育伊,张德楠,孙英杰,张中峰,周龙武,段春燕(1491)

缙云山4种森林植被土壤团聚体有机碳分布特征.....王富华,吕盛,黄容,高明,王子芳,徐畅(1504)

大气污染对居民健康影响研究进展.....秦耀辰,谢志祥,李阳(1512)

《环境科学》征订启事(1042) 《环境科学》征稿简则(1162) 信息(1208, 1235, 1286)

# BiOCl-(NH<sub>4</sub>)<sub>3</sub>PW<sub>12</sub>O<sub>40</sub> 复合光催化剂制备及其光催化降解污染物机制

张文海<sup>1</sup>, 吉庆华<sup>2,3</sup>, 兰华春<sup>2,3</sup>, 李静<sup>1\*</sup>

(1. 河北工业大学土木与交通学院, 天津 300401; 2. 清华大学水质与水生态研究中心, 北京 100084; 3. 中国科学院生态环境研究中心, 北京 100085)

**摘要:** 光生电子和空穴的分离效率是影响光催化性能的重要因素. 氯氧铋是典型的层状纳米光催化剂, 却因光生电子和空穴的快速复合所表现出的低量子效率而受到使用限制. 本文通过两步的水热法合成了 BiOCl-(NH<sub>4</sub>)<sub>3</sub>PW<sub>12</sub>O<sub>40</sub> 复合光催化剂. 以甲基橙(MO)为模拟污染物进行光催化活性测试. 结果表明, 在氙灯模拟的太阳光照射下, Bi 与 W 的原子比为 1:1 时, 其催化效果最佳. 通过自由基猝灭实验对催化剂降解 MO 的催化机制进行了研究, 发现 BiOCl 是由空穴, 羟基自由基和超氧自由基共同作用来对 MO 进行降解; 而复合催化剂则主要以羟基自由基和超氧自由基为活性物种来降解 MO. 通过对反应前后的催化剂进行 XPS 分析, 证明了磷酸铵可以接收 BiOCl 产生的光生电子. 通过光电流测试, 表明复合光催化剂的光生电子的转移和分离效率有了较大的提高, 从而提高了光催化活性.

**关键词:** BiOCl-NH<sub>4</sub>PTA; 复合光催化剂; 甲基橙; 光生电子受体; 电子空穴分离效率

中图分类号: X131; X703.1 文献标识码: A 文章编号: 0250-3301(2019)03-1295-07 DOI: 10.13227/j.hjxx.201808239

## Preparation of BiOCl-(NH<sub>4</sub>)<sub>3</sub>PW<sub>12</sub>O<sub>40</sub> Photocatalyst and a Mechanism for Photocatalytic Degradation of Organic Pollutants

ZHANG Wen-hai<sup>1</sup>, JI Qing-hua<sup>2,3</sup>, LAN Hua-chun<sup>2,3</sup>, LI Jing<sup>1\*</sup>

(1. School of Civil and Transportation Engineering, Hebei University of Technology, Tianjin 300401, China; 2. Center for Water and Ecology, Tsinghua University, Beijing 100084, China; 3. Research Center for Eco-Environmental Sciences, Chinese Academy of Sciences, Beijing 100085, China)

**Abstract:** The separation efficiency of photogenerated electrons and holes is the key to photocatalytic performance. Layered BiOCl is a kind of newly exploited efficient photocatalyst, but its wide-spread practical application is hindered by the rapid recombination of photogenerated electron-hole pairs and low quantum efficiency. In this study, we prepared a composite photocatalyst via a hydrothermal method in which (NH<sub>4</sub>)<sub>3</sub>PW<sub>12</sub>O<sub>40</sub> (NH<sub>4</sub>PTA) is the acceptor of photoelectrons from BiOCl. The photocatalytic performance of variants of BiOCl-NH<sub>4</sub>PTA was evaluated by the removal efficiency of methyl orange (MO). The experimental results showed that the BiOCl-NH<sub>4</sub>PTA [n(Bi):n(W) = 1:1] had the best photocatalytic activity under the irradiation of sunlight simulated by xenon light. The photocatalytic mechanism was investigated using the reactive species trapping experiments. It was found that MO could be photodegraded by ·OH, and holes over BiOCl. Differently, and ·OH were the dominant reactive species for the reactions over the composite photocatalyst. It was proved that NH<sub>4</sub>PTA was the acceptor of photoelectrons by the XPS on the photocatalyst before and after reaction. The photocurrent test verified the superior photocatalysis of BiOCl-NH<sub>4</sub>PTA which was attributed to the efficient separation of electron-hole pairs.

**Key words:** BiOCl-NH<sub>4</sub>PTA; composite photocatalyst; methyl orange; photoelectrons acceptor; separation efficiency of electron-hole pairs

光催化氧化技术作为高级氧化技术的一种, 在处理难降解有机污染物方面表现良好. 而光生电子和空穴的重组, 极大影响了光催化的效率, 从而限制了光催化技术的应用<sup>[1]</sup>.

BiOCl 是典型的铋系半导体光催化材料, 具有特殊的晶体和电子结构, [Bi<sub>2</sub>O<sub>2</sub>]<sup>2+</sup> 层在两个 Cl 离子层中间. Cl 与 Bi 原子之间共价作用强, 导致 BiOCl 极化率强, 从而决定了较强的内部电场, 一定程度上有利于光生电子-空穴有效分离<sup>[2,3]</sup>, 因此表现出良好的光催化活性. 为进一步降低其光生电子和空穴的复合率, 科研人员不断对其进行改性. 针对 BiOCl 的微结构调制, 有一维纳米线(棒)、二

维纳米片<sup>[2,4]</sup>、三维分层结构<sup>[5,6]</sup> 和支撑薄膜<sup>[7,8]</sup> 四大类. 针对 BiOCl 的复合催化剂, 有半导体复合<sup>[9,10]</sup>、金属复合<sup>[11,12]</sup>、助催化敏化<sup>[13,14]</sup> 三大类. 针对 BiOCl 的结构设计, 有掺杂或缺陷引入<sup>[15,16]</sup>、固溶体光催化剂<sup>[17,18]</sup> 和其它卤代铋光催化剂<sup>[19,20]</sup> 三大类. 这些改性对光催化活性有了明显的提升.

为了使光生电子得以迅速转移从而降低光生电

收稿日期: 2018-08-29; 修订日期: 2018-09-19

基金项目: 国家水体污染控制与治理科技重大专项(2017ZX07202003); 河北省住房和城乡建设厅科研项目(2014-230)

作者简介: 张文海(1993~), 男, 硕士研究生, 主要研究方向为光催化降解有机污染物, E-mail: zwhxs1024@163.com

\* 通信作者, E-mail: tdhjlj@163.com

子和空穴的复合,人们可以为其添加一种电子受体.多金属氧酸盐分子体积巨大,结构确定,并且具有质子储存和转移的能力,而且还原态和氧化态的多酸不会因为得失电子而导致结构变形,如已经证实 Keggin 型结构的  $[XM_{12}O_{40}]^{n-}$  能够接受 32 个电子<sup>[21]</sup>并保持结构稳定.由于多金属氧酸盐在一定条件下可以进行可逆的、多步的、多电子的氧化还原过程,因此可以将其作为一类性质优异电子受体. Liu 等<sup>[22]</sup>将磷钨酸与氯化铁形成的  $Fe(III)\{PO_4[WO(O_2)_2]_4\}$  负载到了  $g-C_3N_4$  的表面,在太阳光照条件下,对罗丹明 B 的降解效果良好. Heng 等<sup>[23]</sup>制作的  $H_3PW_{12}O_{40}/TiO_2-In_2S_3$  复合光催化剂对吡虫啉有良好的降解效果.

受此启发,人们可以将磷钨酸铵作为氯氧铋的光生电子受体,制作一种新型的复合光催化剂.近期,只有 Wang 等<sup>[24,25]</sup>通过沸石负载溴氧铋和磷钨酸,实现了可见光下良好的催化活性.但是,复合材料光催化效率提升的机制尚不明确.

本文利用两步水热法,制备了磷钨酸铵和氯氧铋复合光催化剂.以甲基橙为模拟污染物,对复合催化剂的光催化活性进行测试.同时研究了元素配比、不同淬灭剂和酸碱性和对光催化活性的影响.通过淬灭实验、XPS 分析和光电流来对机制进行研究,表明磷钨酸铵可以接受氯氧铋产生的光生电子,使得复合光催化剂的光生电子和空穴复合率有了明显的降低.

## 1 材料与方法

### 1.1 试剂与仪器

主要试剂:硝酸铋  $Bi(NO_3)_3 \cdot 5H_2O$ 、聚乙烯吡咯烷酮(PVP)、甘露醇、饱和 NaCl 溶液、磷钨酸 ( $H_3PW_{12}O_{40} \cdot xH_2O$ )、氯化铵 ( $NH_4Cl$ )、甲基橙(MO)溶液等,以上试剂均为分析纯,实验用水为去离子水.

主要仪器:紫外可见分光光度计(U-3900 日本 Hitachi High-Technologies Co.)、X 射线衍射仪(D8 focus 德国 Bruker 公司)、场发射扫描电子显微镜(SU-8020 日本日立公司)、透射电子显微镜(JEM-2100 日本电子株式会社)、X 射线光电子能谱仪(ESCALAB250Xi 赛默飞世尔科技(中国)有限公司)、红外光谱仪(TENSON 27 BRUKER, Germany)、电化学工作站(Reference 600 + GAMRY).

### 1.2 催化剂制备:

磷钨酸铵  $[(NH_4)_3PW_{12}O_{40}]$  制备:将 300 mg 的  $H_3PW_{12}O_{40} \cdot xH_2O$  和 110 mg 的  $NH_4Cl$  分别溶于 20

mL 和 10 mL 去离子水中,分别记为 A 和 B 溶液(保证  $NH_4Cl$  和  $H_3PW_{12}O_{40} \cdot xH_2O$  的摩尔比大于 3:1).在磁力搅拌的作用下,将 B 溶液缓慢滴加至 A 溶液,搅拌均匀后放入反应釜中,在 140℃ 条件下加热 12 h.自然冷却后通过离心获得沉淀,用去离子水清洗 3 次,再进行冷冻干燥.

复合催化剂制备:参考 Guan 等<sup>[26]</sup>的方式由溶剂热法制备  $BiOCl$ .将 0.486 g 的  $Bi(NO_3)_3 \cdot 5H_2O$  和 0.400 g 的 PVP 溶于 25 mL 的  $0.1 mol \cdot L^{-1}$  的甘露醇溶液,通过超声和机械搅拌使其溶解.加入 5 mL 的饱和 NaCl 溶液,产生均一的白色悬浮液.搅拌 10 min 后,再加入一定比例的磷钨酸铵,搅拌均匀后,倒入到聚四氟乙烯高压反应釜中,放入烘箱中 160℃ 反应 3 h.待反应釜自然冷却到室温后,离心获得固体沉淀物,用去离子水洗涤 3 次以除去多余的离子.样品经过干燥即可使用.

### 1.3 光催化活性测试

催化剂活性以甲基橙(MO)的降解速率来作为评价指标.模拟污染物 MO 的浓度为  $10 mg \cdot L^{-1}$ ,体积为 100 mL,置于 300 mL 烧杯中,加入一定量的催化剂.在磁力搅拌的条件下,利用氙灯模拟太阳光进行光催化实验.反应前,避光吸附 30 min,达到吸附脱附平衡.光照一定时间后取 5 mL 反应液,高速离心分离,用分光光度计在 466 nm 处测其上层清液的吸光度.以溶液的降解率来评价光催化剂的活性,即  $c_t/c_0 = A_t/A_0$  (式中,  $A_t$  和  $A_0$  分别表示  $t$  时间和初始溶液的吸光度).在 pH 条件实验中,利用  $0.5 mol \cdot L^{-1}$  的  $HNO_3$  溶液和  $0.5 mol \cdot L^{-1}$  的 NaOH 溶液调节 pH 值.

## 2 结果与讨论

### 2.1 催化剂理化性质表征

利用 XRD 对  $BiOCl$  和复合催化剂进行分析(图 1).水热法制备的  $BiOCl$  与 JCPDS (No. 82-0485) 相对应.主要以 001 晶面 ( $12.025^\circ$ )、101 晶面 ( $25.905^\circ$ )、110 晶面 ( $32.551^\circ$ ) 和 102 晶面 ( $33.520^\circ$ ) 为主.水热法制备的复合催化剂其峰值与  $BiOCl$  较为吻合,但是却无明显的磷钨酸铵的衍射峰.可能是由于磷钨酸铵的含量相对较少,且分散性较好,致使其无明显的 XRD 特征峰.催化剂反应前后的 XRD 峰值无明显变化,表明催化剂较为稳定.

催化剂的微观结构对催化反应有一定的影响.所以通过 TEM 来对复合催化剂进行微观分析.从图 2(a)看到  $NH_4PTA$  呈球状,粒径大约为 700 nm;图 2(b)中的  $BiOCl$  呈二维薄片状;图 2(c)和图 2

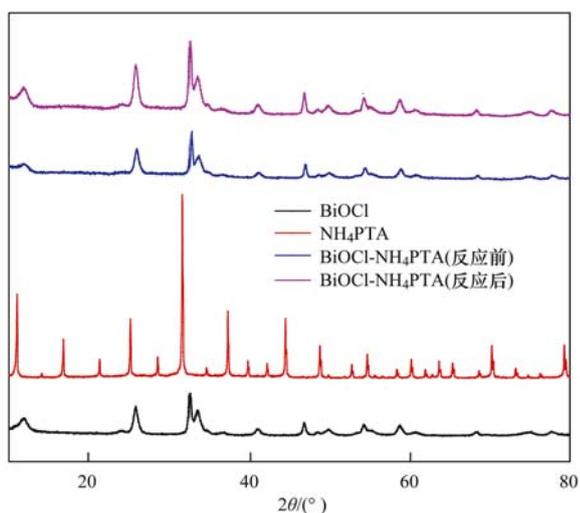


图1 样品 XRD 图

Fig. 1 XRD patterns of samples

(d) 可以看到  $\text{BiOCl}$  纳米片在  $\text{NH}_4\text{PTA}$  上形成了部分的片层覆盖. 图 2(e) 为能谱分析的选定区域, 图 2(f) ~ 2(h) 分别表示为选定区域中的 Bi、W 和 P

元素. 因此可以表明  $\text{NH}_4\text{PTA}$  和  $\text{BiOCl}$  复合良好.

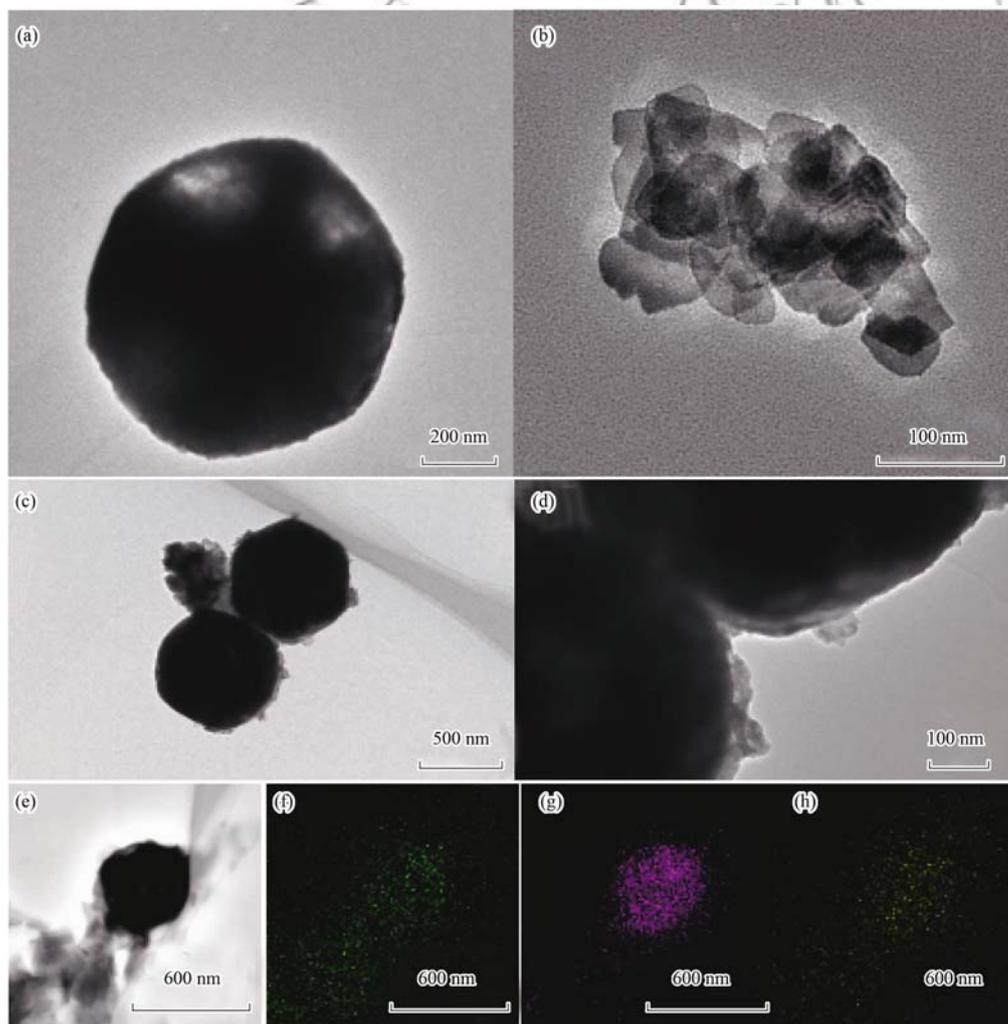
## 2.2 材料光催化活性分析

### 2.2.1 磷钨酸铵掺杂比

在氙灯模拟的太阳光条件下, 不同掺杂比例的  $\text{BiOCl}-\text{NH}_4\text{PTA}$  复合光催化剂对 MO 降解进行了比较实验. 如图 3(a) 所示, 引入磷钨酸铵后, 催化降解速率较  $\text{BiOCl}$  有了明显的提升, 当 Bi 与 W 的摩尔比 1:1 时, 对 MO 的光催化效果最佳, 在光照 0.5 h 后, MO 的降解率达到了 90% 以上. 不同掺杂比例的  $\text{BiOCl}-\text{NH}_4\text{PTA}$ , 其降解速率也有所区别. 这可能是由于  $\text{BiOCl}$  过多, 会对  $\text{NH}_4\text{PTA}$  过分包裹, 从而降低了光生电子的传递. 后续实验中, 均选用催化效果最好的  $\text{BiOCl}-\text{NH}_4\text{PTA}$  [ $n(\text{Bi}):n(\text{W}) = 1:1$ ] 进行实验.

### 2.2.2 pH 对光催化影响

本实验中, 利用  $0.5 \text{ mol}\cdot\text{L}^{-1}$  的  $\text{NaOH}$  溶液和  $0.5 \text{ mol}\cdot\text{L}^{-1}$  的  $\text{HNO}_3$  来调节反应体系的 pH 值. 通过图 3(b) 可以看到, 在酸性条件下降解效果较好.



(a)  $\text{NH}_4\text{PTA}$  透射电镜图; (b)  $\text{BiOCl}$  透射电镜图; (c) 和 (d)  $\text{BiOCl}-\text{NH}_4\text{PTA}$  的透射电镜图; (e) ~ (h)  $\text{BiOCl}-\text{NH}_4\text{PTA}$  的元素分布

图2 催化剂的透射电镜图和元素分布

Fig. 2 TEM images and element mapping of samples

但是 pH = 10 时, 催化效率很低. 酸碱条件下催化效率的差异是由于酸性条件下, 催化剂表面的正电荷会吸引光生电子迁移到催化剂表面, 一定程度上

加强了光生电子和空穴的分离; 同时, 迁移到催化剂表面的电子可以与水中的  $O_2$  反应生成超氧自由基, 进而提高光催化降解的效率<sup>[27,28]</sup>.

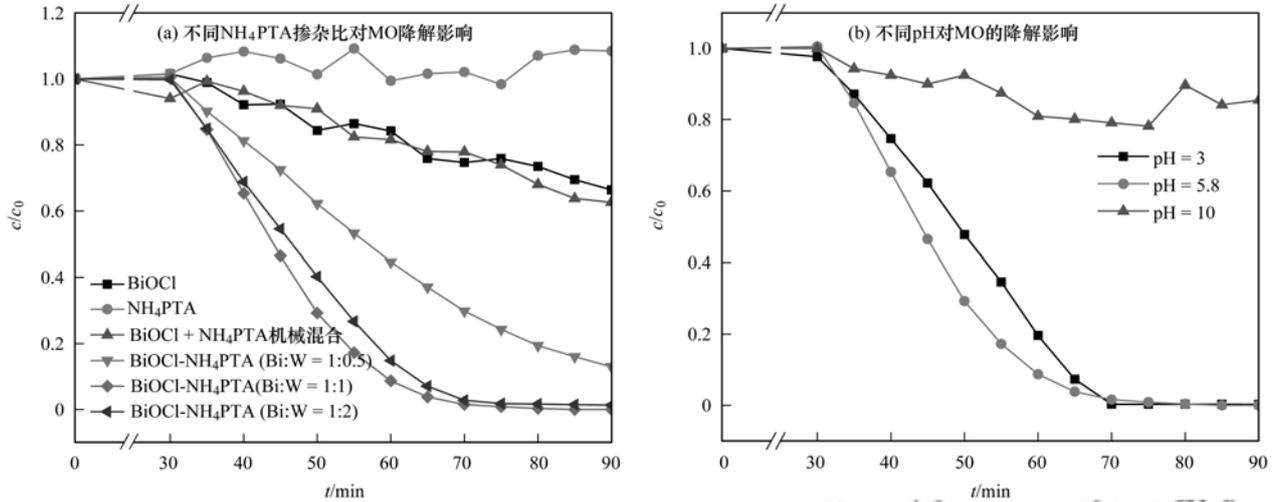


图 3 催化剂对甲基橙的降解效果

Fig. 3 Image of degradation effects of different photocatalysts for MO

### 2.3 降解机制讨论

紫外可见漫反射吸收光谱可以直观地显示材料在不同波长下的光吸收值. 如图 4(a) 所示, 复合催化剂较 BiOCl 发生了明显的红移, 表明复合催化剂增强了可见光区的吸收, 可以利用更多波长范围的光, 进而在实际条件的运用有了一定的基础. 异质结的形成, 会对物质的能带产生一定的影响. 所以通过计算对比了二者的禁带宽度. 根据 Tauc plot 公式:

$$(\alpha hv)^{1/n} = A(hv - E_g)$$

式中,  $\alpha$  为吸光指数,  $h$  为普朗克常数,  $v$  为频率,  $A$  为常数,  $E_g$  为半导体禁带宽度. 指数  $n$  与半导体类型有关. 直接带隙半导体:  $n = 1/2$ ; 间接带隙半导体  $n = 2$ . BiOCl 是间接带隙半导体, 故  $n$  取 2. 由此以  $(Ahv)^{0.5}$  对  $hv$  作图, 其结果如图 4(b) 所示, 计算

可得 BiOCl 和复合催化剂的禁带宽度值分别为 2.99 eV 和 2.07 eV. 禁带宽度的减小, 可以使催化剂利用更多长波段的光, 进行催化反应.

为探究光催化降解 MO 的内在机制, 通过自由基淬灭实验来对反应过程中的活性物种进行研究. 本实验中, 以甲醇为空穴淬灭剂, 叔丁醇作为羟基自由基淬灭剂, Ar 曝气来抑制超氧自由基的生成. 图 5 分别为 BiOCl 和复合催化剂的淬灭实验结果. 在 BiOCl 降解 MO 的过程中, 空穴、羟基自由基和超氧自由基淬灭后, 其反应速率均有明显的下降, 说明以上 3 种活性物种均参与了反应. 在复合催化剂的降解 MO 的过程中, 羟基自由基和超氧自由基淬灭后, 反应速率有明显的下降, 而空穴的淬灭对反应速率的影响较小, 说明 BiOCl- $NH_4PTA$  复合材料降解 MO 主要通过羟基自由基和超氧自由基.

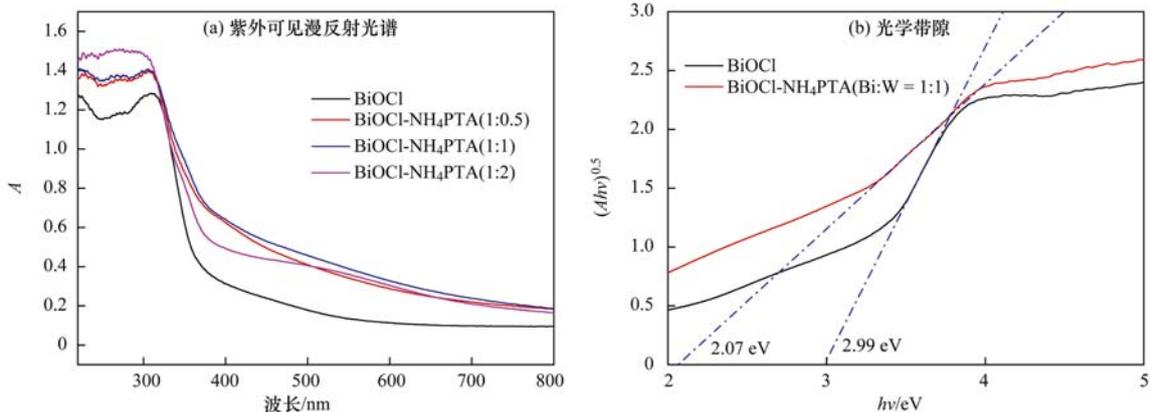
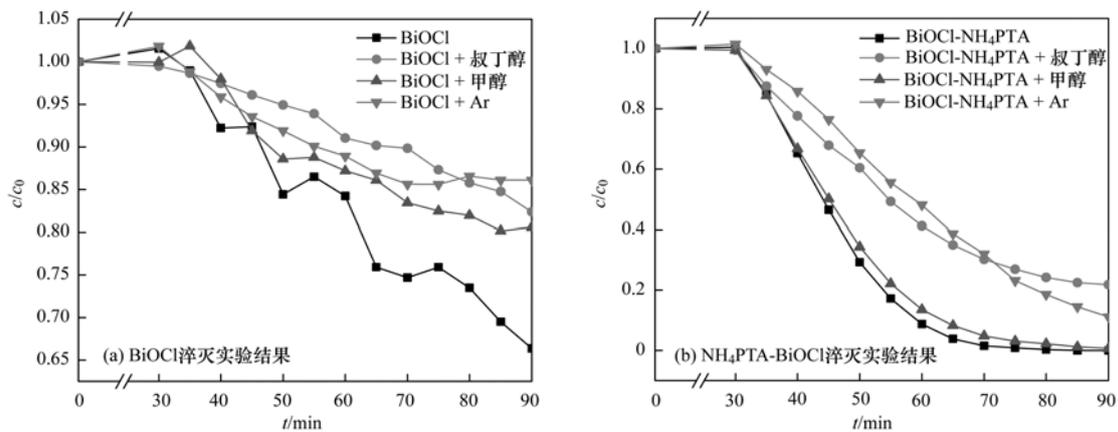


图 4 BiOCl 和  $NH_4PTA$ -BiOCl 的光学性质

Fig. 4 Optical properties of BiOCl and  $NH_4PTA$ -BiOCl

图5 BiOCl 和 NH<sub>4</sub>PTA-BiOCl 光催化氧化 MO 反应机制Fig. 5 Reaction mechanism of BiOCl and NH<sub>4</sub>PTA-BiOCl in the photocatalytic oxidation of MO

XPS 是分析元素价态和化学环境的重要手段之一. 为了分析氯氧铋和磷钨酸铵的结合方式, 本研究对 BiOCl 和复合催化剂中的 Bi 元素进行了 XPS 分析, 其结果如图 6(a) 所示. 158.93 eV 和 164.24 eV 对应着 Bi4f 轨道, 表明铋元素为 +3 价<sup>[29]</sup>. 复合催化剂的 Bi4f 元素的结合能偏移到了 159.20 eV 和 164.55 eV, 表明 BiOCl 和磷钨酸铵形成了强烈的化学键, 而不是二者简单的机械混合<sup>[30,31]</sup>. 为了验证复合材料反应后磷钨酸铵是否得电子, 本研究对反应前后催化剂的钨元素进行

了 XPS 分析, 如图 6(b) 所示, 为催化剂反应前后 W4f 轨道电子的结合能. 反应前的 38.17 eV 和 36.05 eV 分别对应着 W4f<sub>5/2</sub> 和 W4f<sub>7/2</sub> 轨道电子的结合能, 表明钨元素为 +6 价<sup>[32]</sup>. 而反应后, 其对应的峰值偏移到了 37.85 eV 和 35.70 eV. XPS 谱图中, 轨道电子向小的结合能方向移动, 表明该元素得电子. 测得的这一微小的偏移是由于磷钨酸铵中 W 元素接收了 BiOCl 在光照激发下产生的光生电子, 使得其 XPS 谱图中 W 元素的结合能降低.

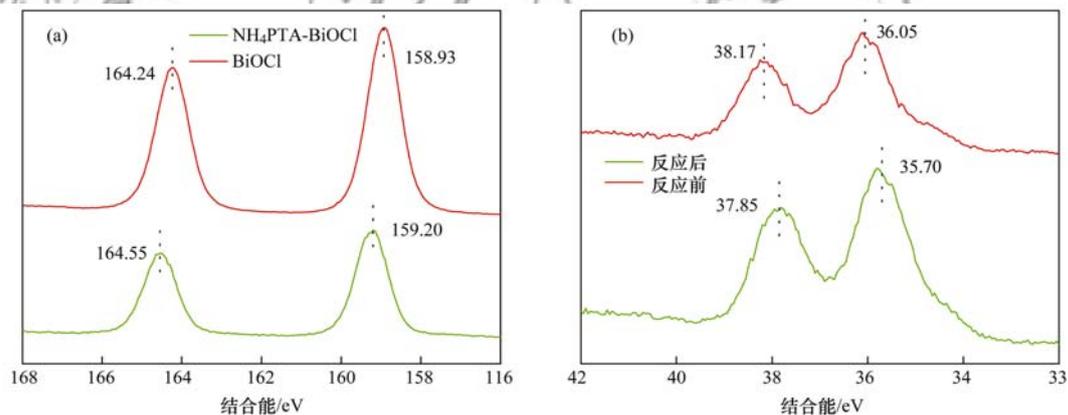
(a) BiOCl 和 NH<sub>4</sub>PTA-BiOCl 中 Bi 元素; (b) NH<sub>4</sub>PTA-BiOCl 催化剂反应前后 W 元素

图6 催化剂 XPS 谱图

Fig. 6 XPS spectra of samples

钨元素微弱的偏移并未整体引起化合价的改变. 如图 7 所示, 在催化反应过程中, 磷钨酸铵接受了来自氯氧铋的光生电子, 传递到磷钨酸铵的电子会迅速与水中的氧气反应, 产生超氧自由基. 该体系在加速分离光生电子和空穴的同时, 产生了具有强氧化性的超氧自由基, 从而提高了光催化活性.

高效的电荷分离和转移是影响光催化的重要因素. 可以通过光电流的测试来验证异质结对光生电

子的分离和迁移影响<sup>[33]</sup>. 在模拟太阳光的照射下, 以 0.1 mol·L<sup>-1</sup> 的 NaSO<sub>4</sub> 溶液为电解液, 在 0.8 V 电压下对 BiOCl 和 BiOCl-NH<sub>4</sub>PTA 进行光电流测试, 其结果如图 8 所示. 在光照时, 可以看到两种类型的光电极都产生了均匀稳定的光电流, 同时光响应具有良好的可逆性. BiOCl 的光电流密度为 0.5 μA·cm<sup>-2</sup>, 复合催化剂 BiOCl-NH<sub>4</sub>PTA 的光电流较 BiOCl 有了明显的提高, 达到了 10 μA·cm<sup>-2</sup>. 光电流的增强是由于复合催化剂的光生电子和空

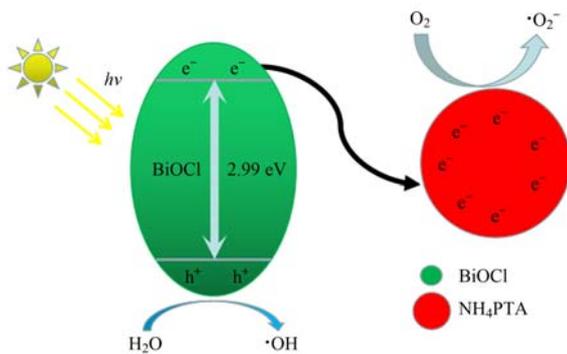
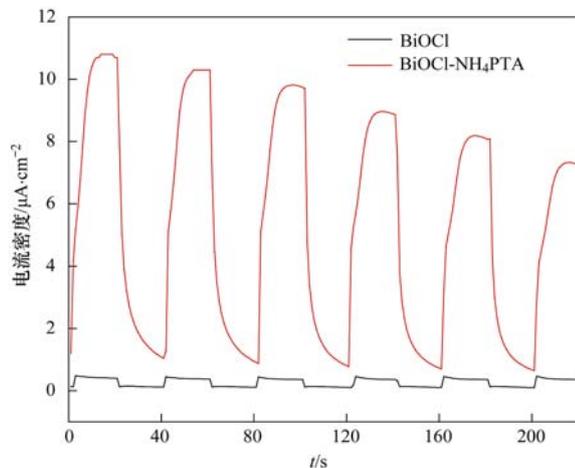


图 7 光生载流子传递示意

Fig. 7 Photo-induced transfer of electrons and holes at the interface between BiOCl and NH<sub>4</sub>PTA图 8 BiOCl 和 BiOCl-NH<sub>4</sub>PTA 的光电流对比Fig. 8 Photocurrent of BiOCl and BiOCl-NH<sub>4</sub>PTA under ultraviolet light

穴可以有效分离<sup>[34]</sup>。

### 3 结论

(1) 通过两步水热法制备了 BiOCl-(NH<sub>4</sub>)<sub>3</sub>PW<sub>12</sub>O<sub>40</sub> 复合光催化剂。当 Bi 与 W 的摩尔比为 1:1 时, 在氙灯模拟的太阳光照射下, 对甲基橙的降解效果最佳。

(2) 通过淬灭实验, 发现羟基自由基和超氧自由基共同作用于光催化氧化过程中。XPS 能谱和光电流测试, 证明了磷钨酸铵作为光生电子受体的作用。磷钨酸铵的引入, 使光生电子和空穴得到了有效地分离。

(3) 将杂多酸作为电子受体引入半导体光催化剂, 将会成为降低光生电子和空穴复合率的一种有效方法。

#### 参考文献:

[ 1 ] Wang H L, Zhang L S, Chen Z G, *et al.* Semiconductor heterojunction photocatalysts: design, construction, and photocatalytic performances [ J ]. *Chemical Society Reviews*, 2014, **43**(15): 5234-5244.  
[ 2 ] Jiang J, Zhao K, Xiao X Y, *et al.* Synthesis and facet-dependent

photoreactivity of BiOCl single-crystalline nanosheets [ J ]. *Journal of the American Chemical Society*, 2012, **134** ( 10 ): 4473-4476.

- [ 3 ] Zhao K, Zhang L Z, Wang J J, *et al.* Surface structure-dependent molecular oxygen activation of BiOCl single-crystalline nanosheets [ J ]. *Journal of the American Chemical Society*, 2013, **135**(42): 15750-15753.  
[ 4 ] Chang X F, Huang J, Cheng C, *et al.* BiOX ( X = Cl, Br, I ) photocatalysts prepared using NaBiO<sub>3</sub> as the Bi source: characterization and catalytic performance [ J ]. *Catalysis Communications*, 2010, **11**(5): 460-464.  
[ 5 ] Zhang X, Ai Z H, Jia F L, *et al.* Generalized one-pot synthesis, characterization, and photocatalytic activity of hierarchical BiOX ( X = Cl, Br, I ) nanoplate microspheres [ J ]. *The Journal of Physical Chemistry C*, 2008, **112**(3): 747-753.  
[ 6 ] Zhu L P, Liao G H, Bing N C, *et al.* Self-assembled 3D BiOCl hierarchitectures: tunable synthesis and characterization [ J ]. *Crystengcomm*, 2010, **12**(11): 3791-3796.  
[ 7 ] Mu Q H, Zhang Q H, Wang H Z, *et al.* Facile growth of vertically aligned BiOCl nanosheet arrays on conductive glass substrate with high photocatalytic properties [ J ]. *Journal of Materials Chemistry*, 2012, **22**(33): 16851-16857.  
[ 8 ] Li Y Y, Liu J P, Jiang J, *et al.* UV-resistant superhydrophobic BiOCl nanoflake film by a room-temperature hydrolysis process [ J ]. *Dalton Transactions*, 2011, **40**(25): 6632-6634.  
[ 9 ] Cheng H F, Huang B B, Qin X Y, *et al.* A controlled anion exchange strategy to synthesize Bi<sub>2</sub>S<sub>3</sub> nanocrystals/BiOCl hybrid architectures with efficient visible light photoactivity [ J ]. *Chemical Communications*, 2011, **48**(1): 97-99.  
[ 10 ] Zhang J, Xia J X, Yin S, *et al.* Improvement of visible light photocatalytic activity over flower-like BiOCl/BiOBr microspheres synthesized by reactable ionic liquids [ J ]. *Colloids and Surfaces A: Physicochemical and Engineering Aspects*, 2013, **420**: 89-95.  
[ 11 ] Li H, Zhang L Z. Oxygen vacancy induced selective silver deposition on the { 001 } facets of BiOCl single-crystalline nanosheets for enhanced Cr(VI) and sodium pentachlorophenate removal under visible light [ J ]. *Nanoscale*, 2014, **6** ( 14 ): 7805-7810.  
[ 12 ] Weng S X, Chen B B, Xie L Y, *et al.* Facile in situ synthesis of a Bi/BiOCl nanocomposite with high photocatalytic activity [ J ]. *Journal of Materials Chemistry A*, 2013, **1**(9): 3068-3075.  
[ 13 ] Gao F D, Zeng D W, Huang Q W, *et al.* Chemically bonded graphene/BiOCl nanocomposites as high-performance photocatalysts [ J ]. *Physical Chemistry Chemical Physics*, 2012, **14**(30): 10572-10578.  
[ 14 ] Zhang L, Wang W Z, Sun S M, *et al.* Water splitting from dye wastewater: a case study of BiOCl/copper(II) phthalocyanine composite photocatalyst [ J ]. *Applied Catalysis B: Environmental*, 2013, **132-133**: 315-320.  
[ 15 ] Pare B, Sarwan B, Jonnalagadda S B. Photocatalytic mineralization study of malachite green on the surface of Mn-doped BiOCl activated by visible light under ambient condition [ J ]. *Applied Surface Science*, 2011, **258**(1): 247-253.  
[ 16 ] Ye L Q, Deng K J, Xu F, *et al.* Increasing visible-light absorption for photocatalysis with black BiOCl [ J ]. *Physical Chemistry Chemical Physics*, 2012, **14**(1): 82-85.  
[ 17 ] Liu Y Y, Son W J, Lu J B, *et al.* Composition dependence of the photocatalytic activities of BiOCl<sub>1-x</sub>Br<sub>x</sub> solid solutions under visible light [ J ]. *Chemistry-A European Journal*, 2011, **17** (34): 9342-9349.

- [18] Ren K X, Liu J, Liang J, *et al.* Synthesis of the bismuth oxyhalide solid solutions with tunable band gap and photocatalytic activities[J]. Dalton Transactions, 2013, **42**(26): 9706-9712.
- [19] Xiao X Y, Jiang J, Zhang L Z. Selective oxidation of benzyl alcohol into benzaldehyde over semiconductors under visible light: The case of Bi<sub>12</sub>O<sub>17</sub>Cl<sub>2</sub> nanobelts[J]. Applied Catalysis B: Environmental, 2013, **142-143**: 487-493.
- [20] Zhai Y F, Zhang A, Teng F, *et al.* Effect of mixed anion layer on energy band, charge separation and photochemical properties of (BiO)<sub>2</sub>OHCl [J]. Applied Catalysis B: Environmental, 2018, **224**: 116-124.
- [21] Launay J P. Reduction de l'ion metatungstate; Stades elevés de reduction de H<sub>2</sub>W<sub>12</sub>O<sub>40</sub><sup>6-</sup>, derives de l'ion HW<sub>12</sub>O<sub>40</sub><sup>7-</sup> et discussion generale [J]. Journal of Inorganic and Nuclear Chemistry, 1976, **38**(4): 807-816.
- [22] Liu J H, Xie S Y, Geng Z B, *et al.* Carbon nitride supramolecular hybrid material enabled high-efficiency photocatalytic water treatments [J]. Nano Letters, 2016, **16**(10): 6568-6575.
- [23] Heng H M, Gan Q, Meng P C, *et al.* The visible-light-driven type III heterojunction H<sub>3</sub>PW<sub>12</sub>O<sub>40</sub>/TiO<sub>2</sub>-In<sub>2</sub>S<sub>3</sub>: a photocatalysis composite with enhanced photocatalytic activity [J]. Journal of Alloys and Compounds, 2017, **696**: 51-59.
- [24] Wang Q Z, Niu T J, Jiao D H, *et al.* Preparation of visible-light-driven BiOBr composites with heteropolyacids (H<sub>3</sub>PW<sub>12</sub>O<sub>40</sub>) encapsulated by a zeolite for the photo-degradation of methyl orange[J]. New Journal of Chemistry, 2017, **41**(11): 4322-4328.
- [25] Wang Q Z, Jiao D H, Bai Y, *et al.* Immobilized heteropolyacids with zeolite (MCM-41) to enhance photocatalytic performance of BiOBr[J]. Materials Letters, 2015, **161**: 267-270.
- [26] Guan M L, Xiao C, Zhang J, *et al.* Vacancy associates promoting solar-driven photocatalytic activity of ultrathin bismuth oxychloride nanosheets [J]. Journal of the American Chemical Society, 2013, **135**(28): 10411-10417.
- [27] Hu L X, Chen F Y, Hu P F, *et al.* Hydrothermal synthesis of SnO<sub>2</sub>/ZnS nanocomposite as a photocatalyst for degradation of Rhodamine B under simulated and natural sunlight [J]. Journal of Molecular Catalysis A: Chemical, 2016, **411**: 203-213.
- [28] Aghdam S M, Haghghi M, Allahyari S, *et al.* Precipitation dispersion of various ratios of BiOI/BiOCl nanocomposite over g-C<sub>3</sub>N<sub>4</sub> for promoted visible light nanophotocatalyst used in removal of acid orange 7 from water [J]. Journal of Photochemistry and Photobiology A: Chemistry, 2017, **338**: 201-212.
- [29] Yan Y, Sun S F, Song Y, *et al.* Microwave-assisted in situ synthesis of reduced graphene oxide-BiVO<sub>4</sub> composite photocatalysts and their enhanced photocatalytic performance for the degradation of ciprofloxacin. [J]. Journal of Hazardous Materials, 2013, **250-251**: 106-114.
- [30] Duo F F, Wang Y W, Fan C M, *et al.* Low temperature one-step synthesis of rutile TiO<sub>2</sub>/BiOCl composites with enhanced photocatalytic activity [J]. Materials Characterization, 2015, **99**: 8-16.
- [31] Wang X J, Wang Q, Li F T, *et al.* Novel BiOCl-C<sub>3</sub>N<sub>4</sub> heterojunction photocatalysts: in situ preparation via an ionic-liquid-assisted solvent-thermal route and their visible-light photocatalytic activities [J]. Chemical Engineering Journal, 2013, **234**: 361-371.
- [32] Rengifo-Herrera J A, Blanco M, Wist J, *et al.* TiO<sub>2</sub> modified with polyoxotungstates should induce visible-light absorption and high photocatalytic activity through the formation of surface complexes [J]. Applied Catalysis B: Environmental, 2016, **189**: 99-109.
- [33] Zhang G Q, Li X Y, Zheng S Z, *et al.* Construction of TiO<sub>2</sub> nanobelts-Bi<sub>2</sub>O<sub>4</sub> heterojunction with enhanced visible light photocatalytic activity [J]. Colloids and Surfaces A: Physicochemical and Engineering Aspects, 2018, **548**: 150-157.
- [34] Wang Y J, Shi R, Lin J, *et al.* Enhancement of photocurrent and photocatalytic activity of ZnO hybridized with graphite-like C<sub>3</sub>N<sub>4</sub> [J]. Energy & Environmental Science, 2011, **4**(8): 2922-2929.

## CONTENTS

Contribution Assessment of Meteorology Conditions and Emission Change for Air Quality Improvement in Beijing During 2014-2017	YIN Xiao-mei, LI Zi-ming, XIONG Ya-jun, <i>et al.</i>	(1011)
Using Multiple Linear Regression Method to Evaluate the Impact of Meteorological Conditions and Control Measures on Air Quality in Beijing During APEC 2014	LI Ying-ruo, WANG Jun-xia, HAN Ting-ling, <i>et al.</i>	(1024)
Source Apportionment of PM <sub>2.5</sub> in Suburban Area of Beijing-Tianjin-Hebei Region in Autumn and Winter	WANG Tong, HUA Yang, XU Qing-cheng, <i>et al.</i>	(1035)
Fine Particulate Matter Source Profile of Typical Industries in Sichuan Province	FENG Xiao-qiong, CHEN Jun-hui, XIONG Wen-peng, <i>et al.</i>	(1043)
Source Apportionment and Pollution Characteristics of PM <sub>2.5</sub> During the Two Heavy Pollution Episodes in the Winter of 2016 in a Typical Logistics City	ZHAO Xue-yan, YANG Wen, WANG Jing, <i>et al.</i>	(1052)
Pollution Characteristics and Source Apportionment of PM <sub>2.5</sub> in Heating and Non-heating Periods in Shenyang	ZHANG Xian, TIAN Sha-sha, LIU Ying-ying, <i>et al.</i>	(1062)
Interannual Variation of Metal Elements and Water-Soluble Ions in PM <sub>2.5</sub> During Wintertime in Xinxiang and Their Source Apportionment	YAN Guang-xuan, LEI Hao-jie, ZHANG Jing-wen, <i>et al.</i>	(1071)
Pollution Characteristics and Source Apportionment of Ambient PM <sub>2.5</sub> During Four Seasons in Yantai City	LIU Tong, WANG Xiao-jun, CHEN Qian, <i>et al.</i>	(1082)
Day-night Characteristics of Humic-like Substances in PM <sub>2.5</sub> During Winter in Changzhou	GU Yuan, LI Qing, HUANG Wen-qian, <i>et al.</i>	(1091)
Pollution Characteristics and Occupational Exposure Risk of Heavy Metals in Indoor and Outdoor Ambient Particles at a Scaled Electronic Waste Dismantling Plant, Northwest China	CAO Hong-mei, ZHAO Liu-yuan, MU Xi, <i>et al.</i>	(1101)
Analysis of a Pollution Process in the Beijing-Tianjin-Hebei Region Based on Satellite and Surface Observations	QIU Yun, LI Ling-jun, JIANG Lei, <i>et al.</i>	(1111)
Spatial-temporal Variation of Ozone Concentration and Its Driving Factors in China	HUANG Xiao-gang, ZHAO Jing-bo, CAO Jun-ji, <i>et al.</i>	(1120)
Ozone Spatial-temporal Distribution and Trend over China Since 2013: Insight from Satellite and Surface Observation	ZHANG Qian-qian, ZHANG Xing-ying	(1132)
Characteristics of Ozone Pollution Distribution and Source Apportionment in Zhoushan	WANG Qiao-li, DONG Min-li, LI Su-jing, <i>et al.</i>	(1143)
Establishment of VOCs Emissions Factor and Emissions Inventory from Using of Architectural Coatings in China	GAO Mei-ping, SHAO Xia, NIE Lei, <i>et al.</i>	(1152)
Heterogeneous Oxidation of Secondary Organic Tracers of Isoprene and Toluene by Ozone	HUANG Ya-juan, CAO Gang, ZHU Rong-shu, <i>et al.</i>	(1163)
Inventory and Spatiotemporal Distribution of Ammonia Emission from Agriculture and Animal Husbandry in Lanzhou City	LI Shi-xue, GUO Wen-kai, HE Xin, <i>et al.</i>	(1172)
Analysis of Stable Hydrogen and Oxygen Isotope Characteristics and Vapor Sources of Event-based Precipitation in Chengdu	HU Yue, LIU Guo-dong, MENG Yu-chuan, <i>et al.</i>	(1179)
Diffusive CO <sub>2</sub> Flux Across the Water-air Interface of Reclaimed Shrimp Ponds in the Minjiang River Estuary Based on the TBL Model	ZHANG Yi-fei, YANG Ping, ZHAO Guang-hui, <i>et al.</i>	(1188)
Distribution and Seasonal Variations of Chromophoric Dissolved Organic Matter (CDOM) in the Bohai Sea and the North Yellow Sea	LIU Zhao-bing, LIANG Wen-jian, QIN Li-ping, <i>et al.</i>	(1198)
Sources, Characteristics and Transformation Dynamics of Fluorescent Dissolved Organic Matter in the Silin Reservoir	LAO Xin-yu, YUAN Jie, LIU Yu, <i>et al.</i>	(1209)
Microplastic Pollution of the Beaches in Xiamen Bay, China	LIU Qi-ming, LIANG Hai-tao, XI Gui-li, <i>et al.</i>	(1217)
Biogeochemical Characteristics in Shengli Site of Lijiang River Under the High Resolution Monitoring	WANG Qi-gang, XIAO Qiong, ZHAO Hai-juan, <i>et al.</i>	(1222)
Hydrochemical Characteristics and Possible Controls of Groundwater in the Xialatuo Basin Section of the Xianshui River	HE Jin, ZHANG You-kuan, ZHAO Yu-qing, <i>et al.</i>	(1236)
Pollution Characteristics of OPEs in the Surface Water and Sediment of the Jinjiang River in Chengdu City	WU Di, YIN Hong-ling, LI Shi-ping, <i>et al.</i>	(1245)
Community Structure and Predictive Functional Analysis of Surface Water Bacterioplankton in the Danjiangkou Reservoir	ZHANG Fei, TIAN Wei, SUN Feng, <i>et al.</i>	(1252)
Influence of Cyanobacterial Blooms on Denitrification Rate in Shallow Lake Taihu, China	LIU Zhi-ying, XU Hai, ZHAN Xu, <i>et al.</i>	(1261)
Assessment of Ecosystem Health of an Urban River Based on the Microbe Index of Biotic Integrity (M-IBI)	SU Yao, XU Yu-xin, AN Wen-hao, <i>et al.</i>	(1270)
Influences of Biochar Application on Root Aerenchyma and Radial Oxygen Loss of <i>Acorus calamus</i> in Relation to Subsurface Flow in a Constructed Wetland	HUANG Lei, LIANG Yin-kun, LIANG Yan, <i>et al.</i>	(1280)
Pollution Load Characteristics of Runoff from Urban Roofs of Different Materials	HE Hu-bin, CHEN Cheng, LIN Yu-qing, <i>et al.</i>	(1287)
Preparation of BiOCl-(NH <sub>4</sub> ) <sub>3</sub> PW <sub>12</sub> O <sub>40</sub> Photocatalyst and a Mechanism for Photocatalytic Degradation of Organic Pollutants	ZHANG Wen-hai, JI Qing-hua, LAN Hua-chun, <i>et al.</i>	(1295)
High Efficiency Removal of 1,2-Dichloroethane from Groundwater by Microscale Zero-valent Iron Combined with Biological Carbon Source	WU Nai-jin, SONG Yun, WEI Wen-xia, <i>et al.</i>	(1302)
Removal of Lead Ions from Water by Struvite Natural Zeolite Composite	DEND Man-jun, WANG Xue-jiang, CHENG Xue-jun, <i>et al.</i>	(1310)
Characteristics of Phosphorus Adsorption in Aqueous Solution By Ca/Mg-Loaded Biogas Residue Biochar	YI Man, LI Ting-ting, LI Hai-hong, <i>et al.</i>	(1318)
Preparation of Two Kinds of Biochar and the Factors Influencing Tetracycline Removal from Aqueous Solution	CHENG Yang, SHEN Qi-bin, LIU Zi-dan, <i>et al.</i>	(1328)
Effect of Zirconium-Modified Zeolite Addition on Migration and Transformation of Phosphorus in River Sediments Under Static and Hydrodynamic Disturbance Conditions	YU Yang, LIN Jian-wei, ZHAN Yan-hui, <i>et al.</i>	(1337)
Removal Efficiencies and Mechanism Research on Four Sulfonamides and Their Acetyl Metabolites in a Wastewater Treatment Plant	WANG Da-peng, ZHANG Xian, YAN Chang-zhou	(1347)
Assessing Performance of Pollutant Removal from Municipal Wastewater by Physical and Chemical Methods Based on Membranes	XU Ting, LI Yong, ZHU Yi-jia, <i>et al.</i>	(1353)
Effect of Influent Ammonia Concentration on a Biological Phosphorus Removal Granules System	LI Dong, CAO Mei-zhong, GUO Yue-zhou, <i>et al.</i>	(1360)
Start-up and Performance Recovery of Granular Sludge for Phosphorus Removal and Nitrification	LI Hai-ling, LI Dong, ZHANG Jie, <i>et al.</i>	(1367)
Realization of Short-cut Nitrification in a CAST Process at High Temperature and Its Phosphorus Removal Performance	MA Juan, YANG Rui-chun, YU Xiao-jun, <i>et al.</i>	(1375)
Nitrogen and Phosphorus Removal from Low C/N Municipal Wastewater Treated by a SPNDR System with Different Aeration and Aerobic Times	YUAN Meng-fei, YU De-shuang, GONG Xiu-zhen, <i>et al.</i>	(1382)
ABR Decarbonization-Nitrosation Coupled with ANAMMOX to Treat Municipal Wastewater	LI Tian, CAO Jia-wei, XIE Feng-lian, <i>et al.</i>	(1390)
Start-up Performance and Sludge Characteristics of Single-stage Autotrophic Nitrogen Removal System with Granular Sludge at Low Ammonia Nitrogen Concentration at Room Temperature	XIE Lu-lin, WANG Jian-fang, QIAN Fei-yue, <i>et al.</i>	(1396)
ANAMMOX Reactor with Two Kinds of Inoculated Sludge: Start-up and Kinetics Characteristics	REN Jun-yi, CHEN Lin-yi, LI Hui-chun, <i>et al.</i>	(1405)
Operation Characteristics of the Biofilm CANON Reactor During the Temperature Reduction Process	FU Kun-ming, LIAO Min-hui, ZHOU Hou-tian, <i>et al.</i>	(1412)
Nitrogen Removal Characteristics and Analysis of Microbial Community Structure in an IEM-UF Simultaneous Separation and Denitrification System	LIU Zi-qi, ZHANG Yan, MA Xiang-shan, <i>et al.</i>	(1419)
Effect of Temperature on the Activity Kinetics of <i>Nitrobacter</i>	YU Xue, SUN Hong-wei, LI Wei-wei, <i>et al.</i>	(1426)
Enhancement for Anaerobic Digestion of Waste Activated Sludge Based on Microwave Pretreatment Combined with Zero Valent Iron	NIU Yu-tong, LIU Ji-bao, MA Shuang, <i>et al.</i>	(1431)
Effects of Environmental Factors on Tetracyclines and Macrolides Resistance Genes in Cattle Manure Composting Systems	PENG Jing, WANG Ke, GU Yue, <i>et al.</i>	(1439)
Effect of Environmental Factors on Variation Characteristics of Soil Microbial Respiration and Its Temperature Sensitivity	ZHANG Yan-jun, GUO Sheng-li	(1446)
Response of Soil Respiration and Its Components to Simulated Acid Rain in a Typical Forest Stand in the Three Gorges Reservoir Area	LI Yi-fan, WANG Yu-jie, WANG Bin, <i>et al.</i>	(1457)
Effects of Fertilization on the Nitrogen Residual Amounts and Leaching from Citrus Orchard Soil in the Three Gorges Reservoir Area	WANG Tian, HUANG Zhi-lin, ZENG Li-xiong, <i>et al.</i>	(1468)
Microbial Carbon Source Metabolic Profile in Rice Rhizosphere and Non-rhizosphere Soils with Different Long-term Fertilization Management	NING Zhao, CHENG Ai-wu, TANG Hai-ming, <i>et al.</i>	(1475)
Characterization of Soil Organic Carbon Mineralization Under Different Gradient Carbon Loading in Paddy Soil	TONG Yao-yao, WANG Ji-fei, ZHU Zhen-ke, <i>et al.</i>	(1483)
Soil Organic Carbon Distribution and Components in Different Plant Communities Along a Water Table Gradient in the Huixian Karst Wetland in Guilin	XU Guang-ping, LI Yan-qiong, SHEN Yu-yi, <i>et al.</i>	(1491)
Distribution of Organic Carbon in Soil Aggregates from Four Kinds of Forest Vegetation on Jinyun Mountain	WANG Fu-hua, LÜ Sheng, HUANG Rong, <i>et al.</i>	(1504)
Review of Research on the Impacts of Atmospheric Pollution on the Health of Residents	QIN Yao-chen, XIE Zhi-xiang, LI Yang	(1512)